ELSEVIER

Thermochimica Acta 388 (2002) 227–232

thermochimica acta

www.elsevier.com/locate/tca

Thermal decomposition of energetic materials Part 80. Pyrolysis of 5-nitraminotetrazole salts of group 1 metals and DFT analysis of the volatile MNCO product ($M = Li^+$, Na^+, K^+, Rb^+, Cs^+)

B.C. Tappan, R.W. Beal, T.B. Brill*

Department of Chemistry and Biochemistry, University of Delaware, Newark, DE 19716, USA

Received 1 February 2001; received in revised form 7 March 2001; accepted 7 March 2001

Abstract

Flash pyrolysis of the energetic Group 1 element (Li^+, Na^+, K^+, Rb^+, Cs^+) salts of mono-anionic and di-anionic 5-nitraminotetrazole (5-NATZ) was conducted by T-jump/FTIR spectroscopy under 1 atm Ar. The mono-anionic salts where M = Na, K, Rb, and Cs produced gaseous phase metal isocyanates, MNCO. The di-anionic salts produced a mixture of volatile metal salts: MNCO, M_2CO_3, and MCN, whose amounts depended on M. Taking the spectral data for LiNCO from our previous work, the IR spectral trends, structure, and bonding of MNCO were calculated with density functional theory (DFT).

Keywords: Flash pyrolysis; FTIR spectroscopy; Density functional theory

1. Introduction

Recently, we observed the apparent formation of volatile metal isocyanates, MNCO, while characterizing the flash pyrolysis of several energetic metal salts: Li, Na, and K(NTO) (NTO = 3-nitro-1,2,4-triazol-5-one) and the K, Rb, and Cs salts of picric acid [1]. As a result of this work, the IR spectra for the complete series of gaseous Group 1 isocyanates (MNCO, M = Li–Cs) are now available. In the present paper on the pyrolysis of Group1 element salts of mono- and di-anionic 5-nitraminotetrazole (5-NATZ), we observed not only MNCO vapor but, in some cases, also M_2CO_3 and MCN vapor. To the extent that these volatile metal salts are able to form particles in the gaseous phase, they may be useful for controlling the stability of combustion by damping the acoustic modes in a combustion chamber, such as a rocket motor.

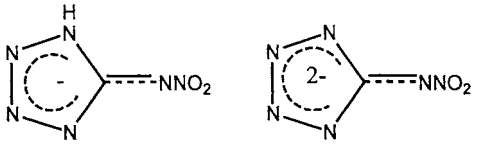

5-NATZ$^-$ 5-NATZ^{2-}

The evidence to date is that MNCO formation is relatively common and not limited to a narrow class of energetic metal salts. As such we sought to

* Corresponding author. Tel.: +1-302-831-6079; fax: +1-302-831-6335.
E-mail address: brill@udel.edu (T.B. Brill).

0040-6031/02/$ – see front matter
PII: S0040-6031(02)00048-5

characterize the structure and bonding of the MNCO series. To our knowledge the previously reported IR spectra of tetra-atomic metallo-pseudohalides in the gaseous phase are limited to NaOCN [2] KOCN [3], and KSCN [3]. In addition, the possible structures of several gaseous metal pseudohalide molecules MXCY, where M = Li, Na, K; X = N, P; and Y = O, S [4–8] have been suggested by ab initio quantum mechanical calculations. The combinations of the lighter non-metal elements were calculated to be lowest in energy as linear molecules, whereas the heavier non-metal elements were proposed to be lowest in energy as a cyclic structure [4–7].

In this paper the flash pyrolysis of the 5-NATZ salts was determined by T-Jump/FTIR spectroscopy and the structure, bonding, and IR spectral features of the gaseous MNCO molecules are described on the basis of density functional theory (DFT) calculations.

2. Experimental

The synthesis and properties of the compounds studied in this paper have been described earlier [9]. T-Jump/FTIR spectroscopy has been described in detail elsewhere [10]. Briefly, about 0.2 mg of sample was thinly spread onto the center of a Pt ribbon filament. The filament was inserted into the cell and the atmosphere was purged with Ar. The IR beam of a Nicolet 20SXC FTIR spectrometer passed about 3 mm above the filament surface. The sample was heated with a filament heating rate of about 2000 °C/sec. The constant set temperatures of the filament depended on the sample. The mono-anionic salts are less thermally stable than the di-anionic salts necessitating filament set temperature in the range of 260–290 °C for the former and the 470–550 °C range for the latter compounds.

Calculations were performed using the Gaussian 98 program package [11]. The geometries were optimized using B3LYP [12] DFT. Few basis sets are available for use with the heavier metals such as K, Rb, and Cs. Calculations based on all of the electrons in these larger atoms require inclusion of highly accurate relativistic effects for the inner shell electrons. This is typically not practical and a suitable alternative approach has been devised in the form of effective core potential (ECP) basis sets. These basis sets consider only a subset of the electrons at or near the valence shell of the atom and model the core electrons based on relativistic calculations. The triple-zeta compact effective potential basis set developed by Stevens et al. (CEP-121) [13] was used for the Li and Na isocyanates, but was not available for the K, Rb and Cs isocyanates. The complete series was calculated with the double zeta Hay–Wadt ECP basis set (LANL2DZ) [14].

It should be noted that the CEP-121 basis set applies a two-electron core potential to all of the atoms in the second row of the Periodic Table. In this case that means that only the 2s and 2p electrons are considered explicitly. Consequently, only one electron is considered in the case of Li. Furthermore, because the third row is assigned an effective core with the electron configuration of Ne, only one electron is again considered explicitly for Na. On the other hand, the Hay–Wadt basis set employs all three electrons of Li, but only one electron for Na. For each Group 1 metal thereafter, nine electrons $[(n-1)s^2(n-1)p^6ns^1]$ are considered.

Although the results of both ECP models on Li and Na were informative, the 6-31 + G* basis set was also tried to compare the results. This is not an ECP basis set and considers all electrons explicitly and also includes polarization and diffusion functions. Good agreement was found between the ECP results and those from the 6-31 + G* basis set. Unfortunately, polarization and diffusion functionality has not been parameterized in Gaussian 98 for the Hay–Wadt basis set beyond Li and Na and so the full set of Group 1 isocyanates could not be compared.

3. Flash pyrolysis results

Each of the 5-NATZ salts was flash pyrolyzed in 1 atm of Ar. Fig. 1 for the salts of the mono-anion and Fig. 2 for the salts of the di-anion reveal significantly different decomposition chemistry. Except for the Li^+ salt, the M(5-NATZ) salts liberate MNCO vapor as the predominant metal-containing species. By comparison the NTO salts of Group 1 elements all produce MNCO [1] except that only small amounts are recorded for the heavier elements. CO_2 and NO occur with variable but mostly small concentrations, the latter of which implies that N_2 must be a major product

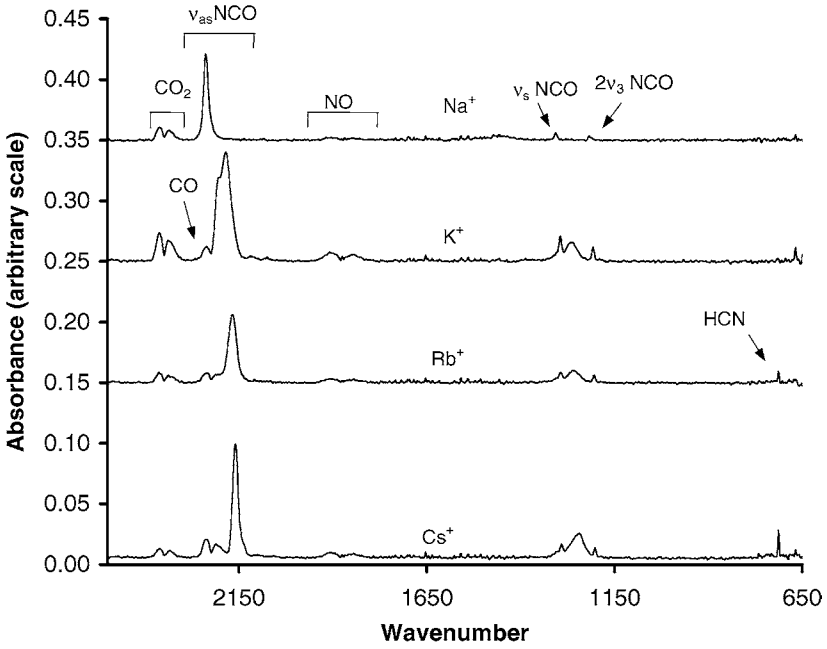

Fig. 1. The mid-IR spectra of the gaseous products following flash pyrolysis of M(5-NATZ) (M = Na, K, Rb, Cs) in 1 atm Ar.

as well. The Li^+ and Na^+ salts of the di-anion favor the formation of MCN, as evidenced by $\nu(CN^-)$ at 2025 and 1988 cm^{-1}, respectively, with a lesser amount of MNCO and/or M_2CO_3, as evidenced by the CO_3^{2-} modes. The frequencies of the carbonate modes of M_2CO_3 are $\nu_{as} = 1553$ and 1473 cm^{-1} (Li^+); 1473 cm^{-1} (Na^+); 1434 cm^{-1} (K^+); 1429 cm^{-1} (Rb^+); and 1422 cm^{-1} (Cs^+). The carbonate bending mode appears at 882 cm^{-1} (Li^+); 881 cm^{-1} (Na^+, K^+, Rb^+); and 880 cm^{-1} (Cs^+).

Eq. (1) is a stoichiometric reaction for flash pyrolysis of the Li and Na salts of the 5-NATZ di-anion,

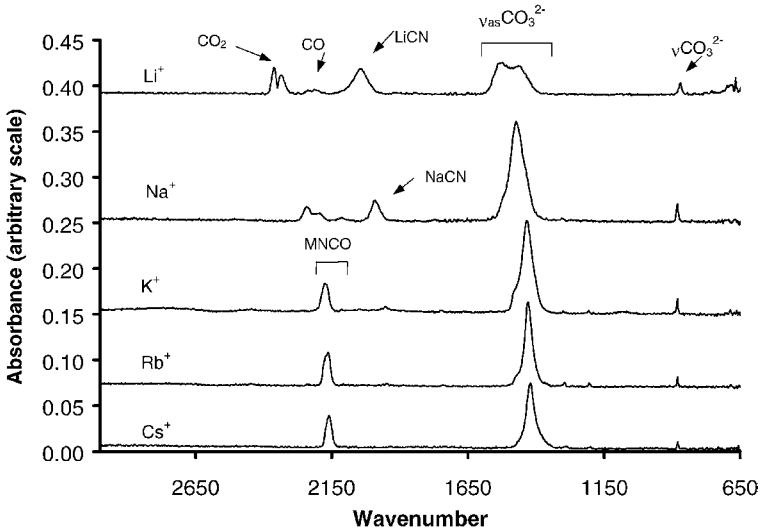

Fig. 2. The mid-IR spectra of the gaseous products following flash pyrolysis of M_2(5-NATZ) where M = Li, Na, K, Rb, Cs in 1 atm Ar.

Table 1
Observed and calculated IR frequencies for gaseous MNCO molecules

M^+	ν_{as} (NCO) (cm^{-1})			ν_s (NCO) (cm^{-1})			$2\nu_3$ (cm^{-1})		
	Observed	CEP-121	LANL2DZ	Observed	CEP-121	LANL2DZ	Observed	CEP-121	LANL2DZ
Li	2254	2241	2227	1320	1365	1326	1220	1296	1208
Na	2234	2220	2204	1304	1324	1274	1218	1296	1196
K	2184		2181	1295		1250	1207		1194
Rb	2169		2178			1243			1190
Cs	2161		2170			1235			1194

while Eq. (2) suitably describes the K, Rb, and Cs salts. These equations are based on qualitative observation, as opposed to quantitation, of the products. The differences are discussed further in the next section.

$$M_2N_6CO_2 \rightarrow \tfrac{2}{3}MCN + \tfrac{1}{3}M_2CO_3 + \tfrac{1}{3}M_2O + \tfrac{8}{3}N_2 + \tfrac{1}{3}O_2 \quad (1)$$

$$M_2N_6CO_2 \rightarrow \tfrac{4}{5}MNCO + \tfrac{2}{5}M_2CO_3 + \tfrac{2}{5}M_2O + \tfrac{13}{5}N_2 + \tfrac{1}{10}O_2 \quad (2)$$

Table 1 gives the IR frequencies for the MNCO compounds in the vapor phase. The data for LiNCO were borrowed from the earlier study of Li(NTO) [1]. Because the K^+ salt has been described earlier, [3] it will be discussed briefly here. Three modes for KNCO are observed in the spectral range studied (Table 1). They agree well with those previously assigned to an authentic sample (2185, 1295, 1207 cm^{-1}) [3], although the KOCN isomer was chosen in [3]. Our interest in understanding: (1) the decrease of the NCO stretching mode frequency with the increase in the mass of the metal M; (2) the differences in the pyrolysis of the salts; and (3) the question of isomeric structures for these tetra-atomic molecules each stimulated an effort to calculate the energies and IR spectral trends of MNCO by quantum chemical methods.

4. DFT calculations

The energies of the MNCO and MOCN isomers were compared in so far as possible using the three basis sets (CEP-121, LANL2DZ and 6-31 + G*). The DFT calculations consistently show that the MNCO isomer is 6–13 kcal/mol lower in energy than the MOCN isomer, and that both are lower in energy than the cyclic structures. This structural finding agrees with recent Hartree–Fock 6-31 + G** calculations for LiNCO and NaNCO [8]. Both ECP models gave differences 1–2 kcal/mol lower than the 6–31 + G* and may underestimate the energy difference between the isomers for the heavier metals as well. Consequently, the linear MNCO isomer was assigned to all of the Group 1 isocyanates. Table 1 contains the IR spectral modes of MNCO calculated with the two ECP basis sets. On the basis of the good agreement between the calculated and observed mid IR frequencies for MNCO, no scaling factor was used in the calculated frequencies in Table 1. The CEP-121 basis set agrees better with the experimental data than does the LANL2DZ basis set, but the trend of decreasing NCO stretching frequency with increasing mass of M is captured in both cases. The apparent origin of this trend is related to both the reduced mass of the atoms in the mode and to the changes in the bonding in the NCO fragment. Fig. 3 is a plot of the reduced mass versus the frequency. This trend has a correlation coefficient (R^2) of 0.968.

A correlation is also found between the NCO stretching frequency and the length of the NCO unit (i.e. the N–O distance) within this series ($R^2 = 0.936$). The distances are shown in Fig. 4. As the mass of M increases, so does the length of the NCO fragment as a result of the increasing ionicity of the M–N bond. This occurrence of course contributes to the decrease in the NCO stretching frequency. The NCO fragment lengthens primarily because of changes in the C–O bond. While the N–C bond maintains an essentially constant length of 1.219 Å (LANL2DZ basis set), the C–O bond lengthens from 1.223 Å for LiNCO to 1.242 Å

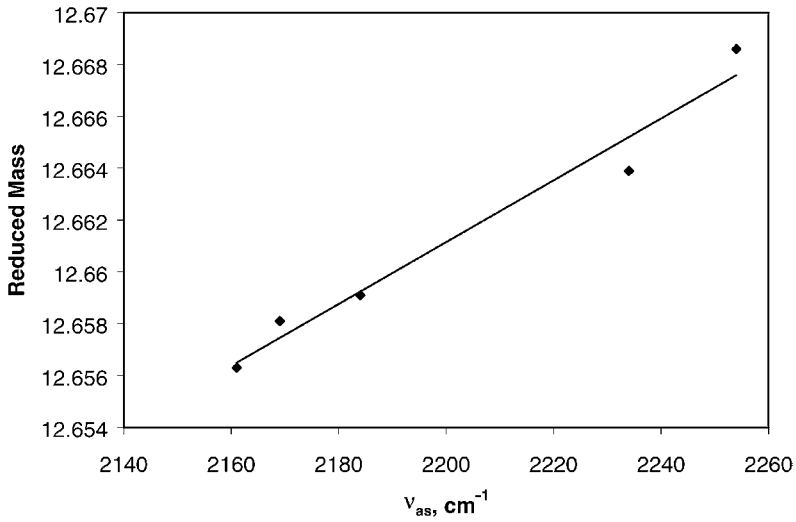

Fig. 3. The relation between the reduced mass of MNCO and the asymmetric NCO stretching frequency.

for CsNCO. The origin of this pattern is revealed in the atom charges (Table 2) that are derived from a Mulliken orbital population analysis. Natural bond orbital analysis was also performed and provides the same trend. As expected, the metal atom develops relatively more positive charge (increased bond ionicity) with the increase in its principal quantum number. As the NCO unit progressively gains negative charge however, the charge on N remains relatively constant, whereas the C and O atoms acquire the increasing negative charge. This is because the non-bonding p-electron density on the O atom dominates the HOMO. This increase in density is further supported by the natural bond orbital analysis. The increased electrostatic repulsion in this part of the molecule lengthens the C–O bond.

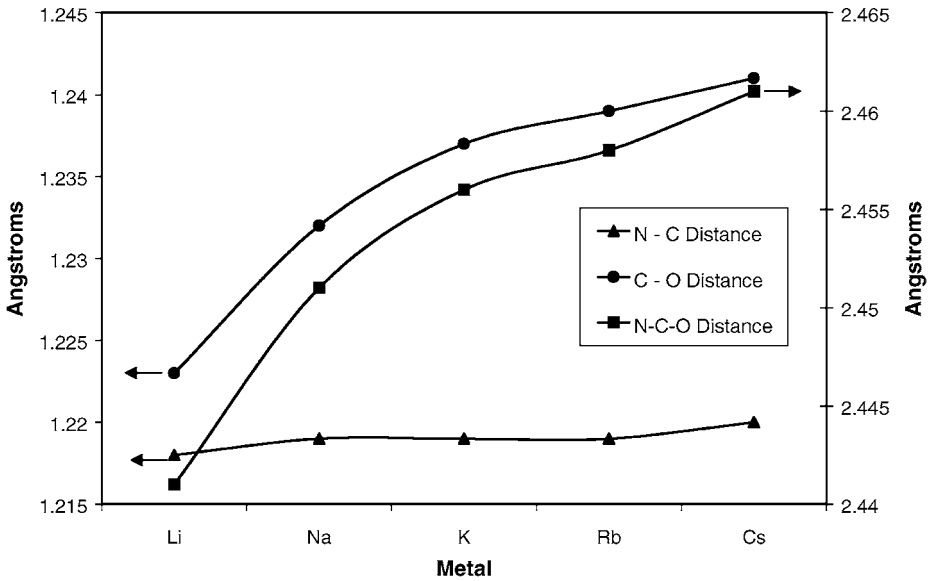

Fig. 4. The distances in the NCO portion of the MNCO molecules as a function of M as calculated by DFT.

Table 2
Calculated atomic charges

	M	N	C	O
Li	0.675	−0.535	0.154	−0.295
Na	0.753	−0.613	0.194	−0.333
K	0.867	−0.571	0.064	−0.360
Rb	0.870	−0.563	0.062	−0.369
Cs	0.888	−0.557	0.047	−0.378

Insight into one of the observations in the preceding section on the difference in the pyrolysis products from the Li^+ and Na^+ salts compared to the K^+, Rb^+, and Cs^+ salts is qualitatively obtained from these DFT calculations. According to Fig. 4 the C–O bond is stronger (shorter) when M = Li and Na compared to M = K, Rb, and Cs. This result suggests that MCN (M = Li and Na) is not formed directly from MNCO, but rather originates directly the decomposition of the M_2(5-NATZ) salt.

Finally, the calculations of the IR spectra in Table 1 permit the atom motions in the normal modes to be identified. The mode labeled ν_1 is predominantly the asymmetric NCO stretch, while ν_2 is predominately the symmetric NCO stretch in which M moves in phase with C, and $2\nu_3$ is the first overtone of the NCO bending mode.

Acknowledgements

TBB is grateful to the Office of Naval Research for support of this work on the MURI program (ONR-N00014-95-1338) as a subcontract from California Institute of Technology. RWB was supported by AFIT, Civilian Institutions.

References

[1] T.B. Brill, T.L. Zhang, B.C. Tappan, Combust. Flame 122 (2000) 165.
[2] Z.K. Ismail, R.H. Hauge, J.L. Margrave, J. Mol. Spectrosc. 45 (1973) 304.
[3] T.C. Devore, J. Mol. Struct. 162 (1987) 273.
[4] T. Pasinszki, T. Veszprémi, M. Fehér, Chem. Phys. Lett. 215 (1993) 395.
[5] T. Veszprémi, T. Pasinszki, M. Fehér, J. Am. Chem. Soc. 116 (1994) 6303.
[6] T. Pasinszki, T. Veszprémi, M. Fehér, THEOCHEM 331 (1995) 289.
[7] T. Pasinszki, T. Veszprémi, M. Fehér, Inorg. Chem. 35 (1996) 2132.
[8] S.S.W. Leung, A. Streitweiser, J. Comput. Chem. 19 (1998) 1325.
[9] B.C. Tappan, C.S. Incarvito, A.L. Rheingold, T.B. Brill, Thermochim. Acta 384 (2002) 113.
[10] T.B. Brill, P.D. Brush, K.J. James, J.E. Shepherd, K.J. Pfeiffer, Appl. Spectrosc. 46 (1992) 900.
[11] M.J. Frisch, G.W. Trucks, H.B. Schlegel, G.E. Scuseria, M.A. Robb, J.R. Cheeseman, V.G. Zakrzewski, J.A. Montgomery Jr., R.E. Stratmann, J.C. Burant, S. Dapprich, J.M. Millam, A.D. Daniels, K.N. Kudin, M.C. Strain, O. Farkas, J. Tomasi, V. Barone, M. Cossi, R. Cammi, B. Mennucci, C. Pomelli, C. Adamo, S. Clifford, J. Ochterski, G.A. Petersson, P.Y. Ayala, Q. Cui, K. Morokuma, D.K. Malick, A.D. Rabuck, K. Raghavachari, J.B. Foresman, J. Cioslowski, J.V. Ortiz, B.B. Stefanov, G. Liu, A. Liashenko, P. Piskorz, I. Komaromi, R. Gomperts, R.L. Martin, D.J. Fox, T. Keith, M.A. Al-Laham, C.Y. Peng, A. Nanayakkara, C. Gonzalez, M. Challacombe, P.M.W. Gill, B. Johnson, W. Chen, M.W. Wong, J.L. Andrers, C. Gonzalez, M. Head-Gordon, E.S. Replogle, J.A. Pople, Gaussian Inc., Pittsburgh, PA, 1998.
[12] P.J. Stephens, F.J. Devlin, C.F. Chabalowski, M.J. Frisch, J. Phys. Chem. 98 (1994) 11623;
A.D. Becke, J. Chem. Phys. 98 (1993) 5648;
C. Lee, W. Yang, R.G. Parr, Phys. Rev. B37 (1988) 785.
[13] W.J. Stevens, M. Krauss, H. Basch, P.G. Jasien, Can. J. Chem. 70 (1992) 612.
[14] P.J. Hay, W.R. Wadt, J. Chem. Phys. 82 (1985) 270.